Proceedings of the 25th International Conference on
Port and Ocean Engineering under Arctic Conditions
June 9-13, 2019, Delft, The Netherlands

ISO 19906 Updates: Global Local Ice Actions

Freeman Ralph[1]
[1] C-CORE, St. John's, Canada

ABSTRACT

As part of a series of papers highlighting updates to the ISO 19906 standard, this paper focuses on global and local ice actions. In particular, more consideration is given to exposure in estimating ice actions as exposure varies from region to region. The Extreme Level (EL) and Abnormal Level (AL) actions are applied directly to local ice conditions rather than reliance on expert judgement. Design expressions in the revised standard are much more transparent providing greater clarity to the designer. Specific updates include: 1) formulations for first-year and multi-year ridge loads on sloping and conical structures to now include updated terms for ridge breaking mechanisms and clearing action; 2) additional background information and data for the limit force formulation for ridge building processes; 3) a correction factor to the global sea-ice pressure equation for narrow structures; 4) consideration for exposure in the global sea-ice pressure equation; 5) consideration for exposure in the deterministic local pressure-area equation for thick massive ice features; 6) the addition of local pressure ship ram data to guide selection of the probabilistic local pressure parameter that varies from region to region; and 7) the addition of a new local pressure clause and probabilistic formulation for long duration continuous interaction events on wide structures.

KEY WORDS

ISO19906; Arctic; Local; Global; Exposure; Probabilistic.

INTRODUCTION

The 2010 edition of the ISO19906 standard has been updated to reflect the latest developments in design to ensure safe and environmentally responsible design for operations in arctic, subarctic and temperate offshore regions where icebergs and sea ice are present. As part of a series of papers to highlight these updates, this paper focuses on global and local ice actions and considers:

- level ice loads on sloping structures;
- multi-year ridge loads on conical structures;
- ridge building pressures;
- global sea ice pressures;
- local ice pressures for massive ice features;
- local design ice pressure for short duration events;
- local design pressures for long duration events; and
- the combination of local ice pressures with global background pressure.

Enhancements were also made to provide more clarity and transparency in the consideration of “exposure” for both deterministic and probabilistic design load estimates since exposure can vary from location to location and depend on when and how the facility is operated. Increased exposure will lead to increased design actions. Available data on ice and environmental conditions is often limited such that maximum observed values are not adequate to estimate EL and AL characteristic actions. Probabilistic methods can often be used in such cases to estimate EL and AL actions based on target safety levels and are therefore less dependent on expert judgement. This too highlights the importance of having sufficient quality data. The revised standard is much more comprehensive and transparent in this regard, providing greater clarity and understanding for the designer.

Before reviewing specific changes with respect to local and global actions, it is useful to highlight the relationship between global and local areas, pressures and loads as it relates to the standard.

GENERAL PRINCIPLES FOR CALCULATING ICE ACTIONS (A.8.2.1)

Global actions represent the total action applied to the structure, whereas the local actions are those applied to a specified area within the nominal contact area. The imprint of the ice feature on the structure at a given penetration, without any reduction for spalls involving pieces of ice that break off, is termed the global or nominal contact area (see Figure 1). The imprint of the ice feature can extend to the full width of the structure. The actual contact area can be much smaller than the nominal contact area.

Smaller areas within the global interaction area can be subjected to high local pressures that are considerably higher than the global average pressures and referred to as High Pressure Zones or HPZs. For local design, the characteristic design ice pressure and action (e.g. as associated with a 10^{-2} annual exceedance probability in the case of AL actions), that can develop on a specific structural area, is required. The highest local pressure on a subarea can occur anytime during the interaction and anywhere within the nominal contact area. A range of local design areas and corresponding local pressures should be evaluated to determine the critical local action for the structure considered.

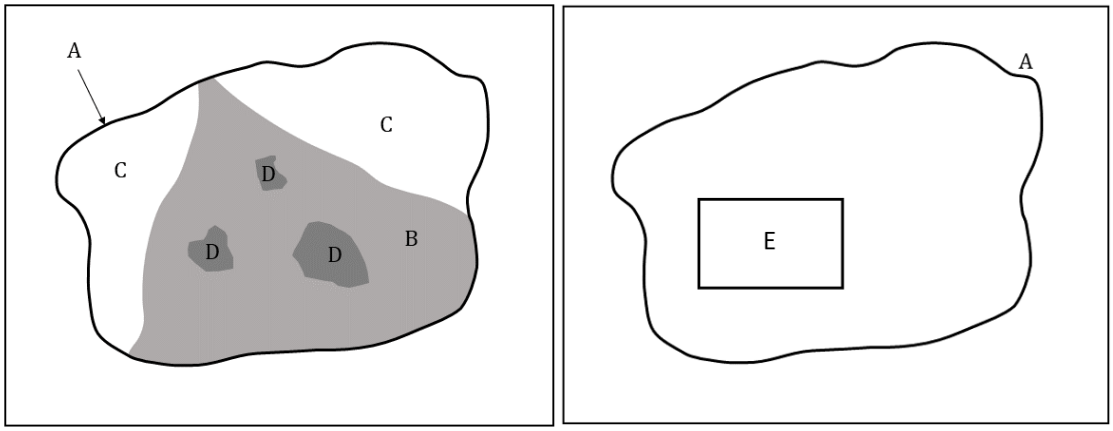

Key

A global interaction area or nominal area
B actual contact area
C large spalled area
D high pressure zones (HPZ)
E design area for local ice actions

Figure 1. Illustration of nominal contact area for glacial or massive ice feature interactions (Figure A.8.2)

GLOBAL PRESSURE FOR SEA ICE (Clause A.8.2.4.3.3)

When ice crushing occurs against a structure, the global ice action normal to the surface, F_G, can be expressed as given in Equation 1 (A.8-19) as

$$F_G = p_G A_N \tag{1}$$

where p_G is the ice pressure averaged over the nominal contact area associated with the global action and A_N is the nominal contact area. This approach is preferable because it is relatively easily to model the nominal area and the actual contact area is not known.

In the earlier version of the standard, upper bound ice pressures for old ice interactions with vertical structures were based on full-scale measurements in the Beaufort Sea, Baltic Sea, Cook Inlet, and Bohai Sea. In the new version of the standard, a new term f_{AR} is added based on observations from relatively narrow bottom-founded lighthouse structures (width <~2 m, ice thickness <~1 m) in the northern Baltic Sea (see Määttänen and Kärnä, 2011). The global ice pressure as a function of ice thickness and width of the structure as estimated in Equation 2 (A.8-21):

$$p_G = C_R \left(\left(\frac{h}{h_1} \right)^n \left(\frac{w}{h} \right)^n + f_{AR} \right) \tag{2}$$

where

p_G is the global average ice pressure, expressed in mega-pascals;
w is the projected width of the structure, expressed in metres;
h is the thickness of the ice sheet, expressed in metres;
h_1 is a reference thickness of 1 m;
m is an empirical coefficient equal to -0.16;
n is an empirical coefficient, equal to -0.50 + h/5 for h < 1,0 m, and to -0.30 for h ≥1,0 m;
C_R is the ice strength coefficient, expressed in mega-pascals
f_{AR} is an empirical term given by

$$f_{AR} = e^{\frac{-w}{3h}} \sqrt{1 + 5\frac{h}{w}}$$

It is noted that data on narrow structures in thicker ice were not available when the term for f_{AR} was developed, so in the absence of other information, the f_{AR} term should be included in global ice pressure calculations.

The influence of f_{AR} is illustrated in the "ISO_enhanced" curve in Figure 2 below.

Three regional values for C_R are specified in Table 1. The C_R value recommended for the Arctic can be conservative, as it potentially includes some magnification due to the compliance of the structure in the referenced data from the Beaufort Sea (Jeffries and Kärnä, 2008).

A new caution has been added in relation to use Equation 2 to address the potential for over conservatism, particularly in the application of reconsolidations layers within a ridge interacting with wide structures. Analyses by Paquette and Brown, (2017) note that C_R values in Table 1 are for different regions and for "undeformed" ice sheets. Using these to estimate ice actions from weaker "deformed" reconsolidated layers of first-year and multi-year ridges, leads to upper bound estimates. The value of C_R can potentially be modified for this scenario based on available data. While it is suggested that the recommended values of C_R, based on regional observations are for EL ice actions, the number and nature of annual events that define exposure can vary from region to region. An alternative probabilistic approach is attractive.

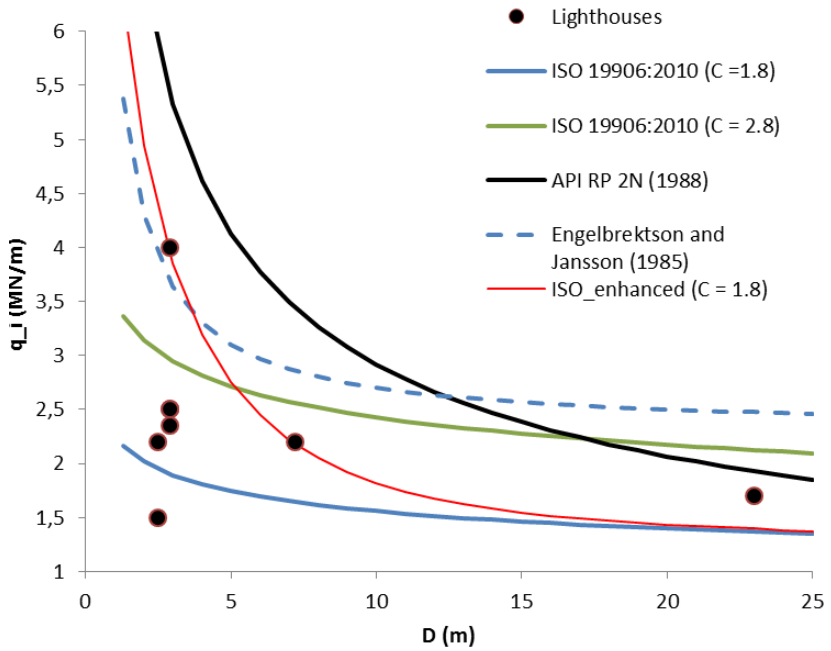

Figure 2. Regional values for ice strength coefficient (Bjerkas and Nord, 2016, Kärnä et al, 2006)

Thijssen and Fuglem (2015) and Thijssen et al. (2016), proposed a probabilistic method for including the effect of exposure on C_R using the temperate ice condition data from the Baltic Sea. Exposure was represented in terms of the distance ice moved past the structure. Using this approach, C_R values are scaled based on exposure and applied to different regions of interest.

Based on Baltic Sea data (see Kärnä, and Qu, 2006), Table 2 illustrates the variability in C_R for different numbers of events per year, n, and for different return periods. As illustrated in the first and second row, n is defined as the annual peak load given approximately 6 km of ice movement. The column identified by $F_P(p)$ is the cumulative probability corresponding to the return period. For a return period of 100 years, the value for C_R would be 1.45. Based on an annual exposure of approximately 135 km of ice movement (or n = 24 events), the C_R value for a 100 return period (i.e. a 10^{-2} annual exceedance probability level) is 1.8.

The specification of ice thickness should consider the annual number of events, which can vary from region to region.

Table 1. Regional values for ice strength coefficient (Table A.8-3)

C_R (MPa)	Region
2.8	Arctic FY and MY ice (e.g. Beaufort)
2.4	Subarctic (e.g. Okhotsk Sea — off northeast Sakhalin Island
1.8	Temperate (e.g. Okhotsk Sea — Aniva Bay, North Caspian Sea, Cook Inlet, Baltic Sea, Bohai Sea)

Table 2. Examples of ice strength coefficient C_R based on exposure (Table A.8-4)

Annual Number of Events n	Associated Total Distance of Ice Movement (km)	Return period	$F_P(p)$	C_R (MPa)
1	6	1 year	0.5	0.99
1	6	100 year	0.99	1.45
24	135	1 year	0.5	1.34
24	135	100 year	0.99	1.8
24	135	10,000 year	0.9999	2.3
100	563	1 year	0.5	1.49
100	563	100 year	0.99	1.96

MULTI-YEAR INTERACTIONS WITH CONICAL STRUCTURES (Clause A.8.2.4.5.2)

New set of deterministic upper bound equations have been developed for multi-year ridge interactions with conical structures. The ridge is assumed to be of rectangular cross section. A formula is given for converting a trapezoidal ridge profile to an equivalent rectangle. The length axis of the ridge is oriented normal to the direction of motion. Physical model tests have shown that obliquely oriented ridges do not give higher actions (Wang et al., 1997). The approach is based on bounding the mechanisms observed in physical tests as well as theoretical reasoning. The mechanisms are:

a) Clearing the debris on the slope from level ice ahead of the ridge (this has to be added to the ridge breaking action, see Figure 3).

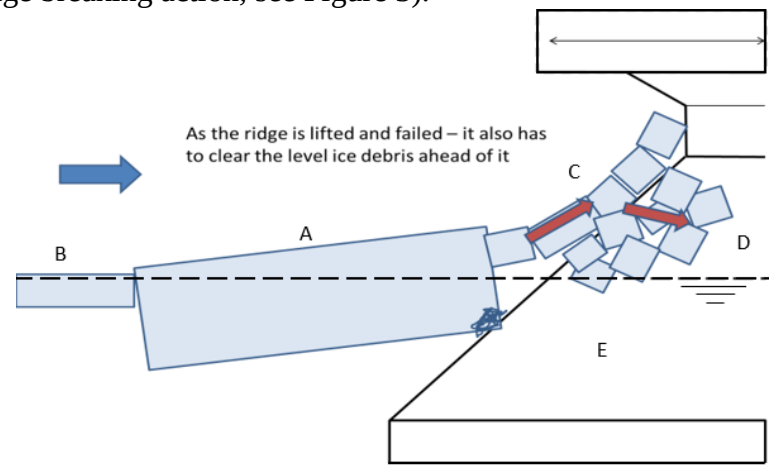

Key

A MY ice ridge
B direction of level ice motion
C ice rubble riding up slope
D ice rubble cleared around structure
E conical structure

Figure 3. Level ice clearing ahead of the ridge (Figure A.8-17)

b) The creation of successive hinge cracks to a length which after the final break will rotate around the structure with no further breaking (this length is specified as $n_R\, h_R$). Based on observations in physical tests and comparison with Masterson (2011) and Nevel, 1992), a value of n_R = 4.5 is recommended. At the lengths corresponding to the final

breaks, the effects of curvature on the elastic foundation modulus can be ignored leading to simplified formulae compared to those of Hetényi (1946), as used in the past.

c) The possibility of the final hinge pieces breaking across the width of the ridge (called z-z failure), see Figure 4.
d) Final clearing of the ice blocks with their leading edge raised to the ridge thickness.

In exercising the approach, it has been found that the introduction of the z-z failures reduces the final clearing action so that over a range of ridge thicknesses, widths and strengths, the controlling action is always that associated with the breaking of the final hinge pieces plus the associated level ice clearing action, (see Croasdale et al., 2016 and Croasdale et al, 2018). This fact leads to a much simplified methodology, which is shown in the logic diagram in Figure 5.

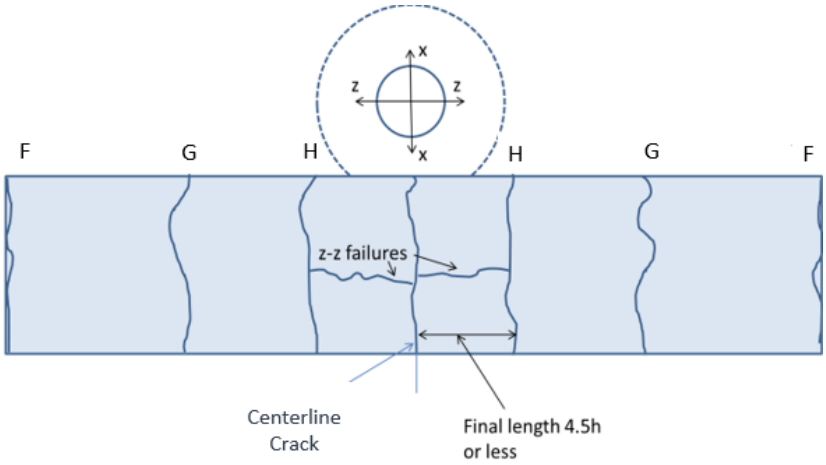

Key

A conical structure
B ice ridge
C level ice
D direction of motion
E center crack, occurs first at lower action
F 1st hinge cracks, one each side
G 2nd hinge cracks, one each side
H possible 3rd hinge cracks, one each side
I z-z failure
l_{3C} final length of broken piece (<4.5 h_R)

Figure 4. Long ridge gradual breaking into smaller hinge lengths with possible final z-z failures (Figure A.8-18)

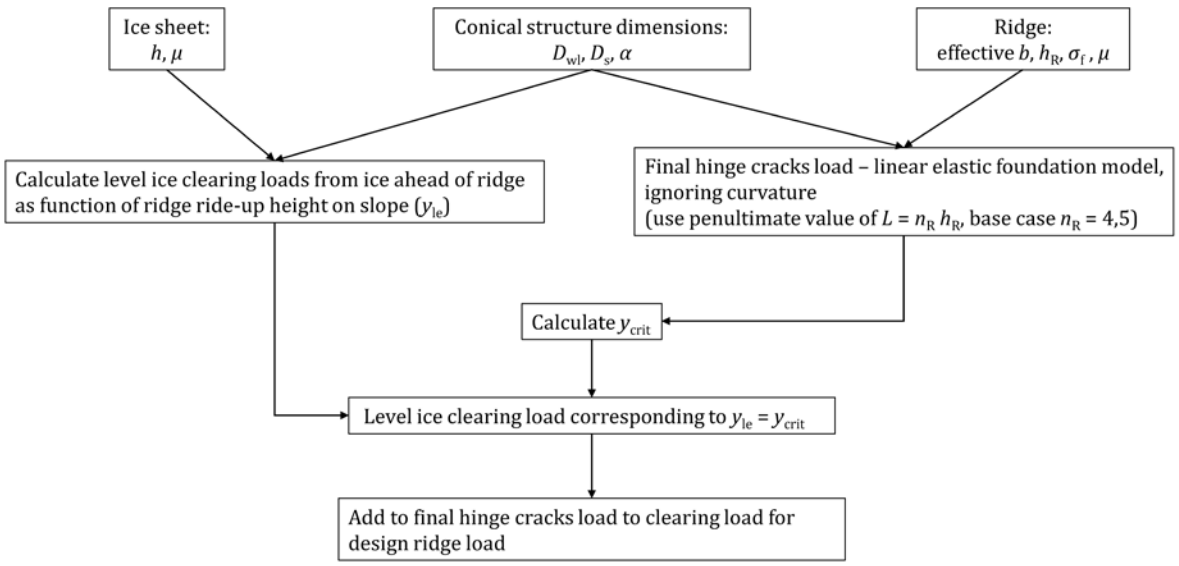

Figure 5. Logic for bounding calculations (Figure A.8-19)

LIMIT FORCE ACTIONS DUE TO RIDGE BUILDING PROCESSES (Clause A.8.2.4.6)

Ice actions due to ridge building (Figure 6) are based on two key parameters; the ridge building action per unit of length, *pD*, on the back of the floe; and the ice feature width, *D*, over which the pack ice is acting. The limit ridge building action is given by Equation 3 (A.8-64):

$$F_B = p_D D \tag{3}$$

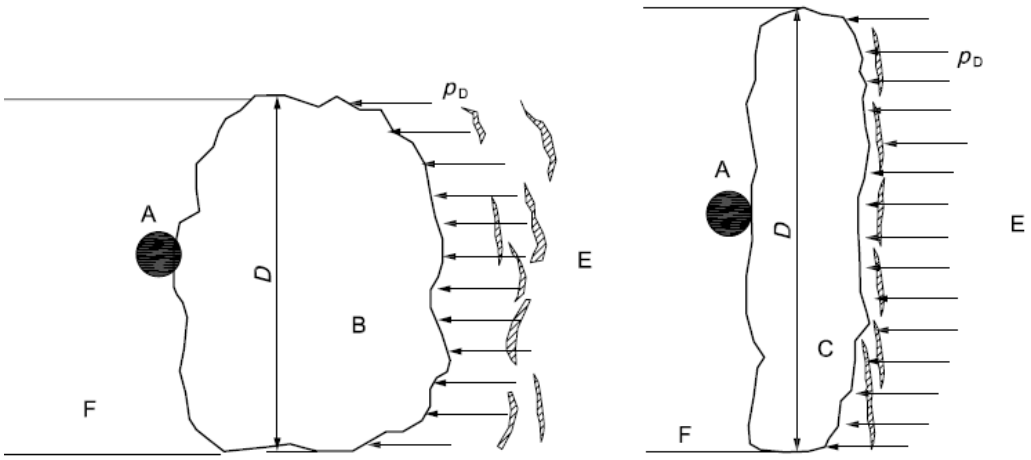

Key

A structure
B thick ice floe
C thick consolidated ice ridge
E surrounding ice sheet
F open water in wake of structure and ice feature
D width of thicker ice feature (m)
p_D line action imposed on the width of the ice feature

Figure 6. Ridge-building action behind thick floe or ridge (Figure A.8-20)

Observations of ridge building and ice rubble building in front of structures indicate that the ice fails with out-of-plane in bending. Figure 7 shows a collection of measured data from rubbling events where first-year ice was failing against a thicker feature. These data include values from sensors embedded in ice floes (Croasdale et al., 1992) values from measurements on Molikpaq, Katie's Floeberg and Hans Island (Sandwell, 1994) and one data point from the Molikpaq where the thicker feature was frozen into the surrounding first year ice (Wright et al., 1992). Ridge building actions were shown to depend on the width, *D*, of the ice feature as illustrated in Figure 7 and given in Equation 4 (A.8-64):

$$p_D = R\, h^{1.25}\, D^{-0.54} \tag{4}$$

where

p_D is the ridge building action per unit width, expressed in meganewtons per metre;
h is the thickness of the ice sheet acting on the thicker ice feature, expressed in metres;
D is the width of the thicker ice feature, expressed in metres;
R is a coefficient (see Figure 7).

In the previous edition of the standard, only the best fit to the data collected from the embedded sensors (Croasdale et al, 1992) was used where $R = 2$. This latest edition includes additional fits to the data; $R = 6$, the best fit to all the data and closely corresponds to the value developed based on theoretical considerations of three ice sheet/rubble interaction mechanisms (Palmer

and Croasdale, 2013, eqn. 5.2.7); and R = 10 passes through the upper bound data points collected for narrower widths (<300m) and for frozen-in floes.

Based on a review of the theories for rubble building and the measured data, it is suggested that, for widths less than 100 m, rubbling failures cannot be relied on and the methodology for crushing actions (see A.8.2.4.3 and A.8.2.4.3.3) should be used. The few data for widths greater than 1500 m suggest a levelling-out of the line actions with width, and applied ridge building line actions should not generally be less than the value corresponding to a width of 1500 m.

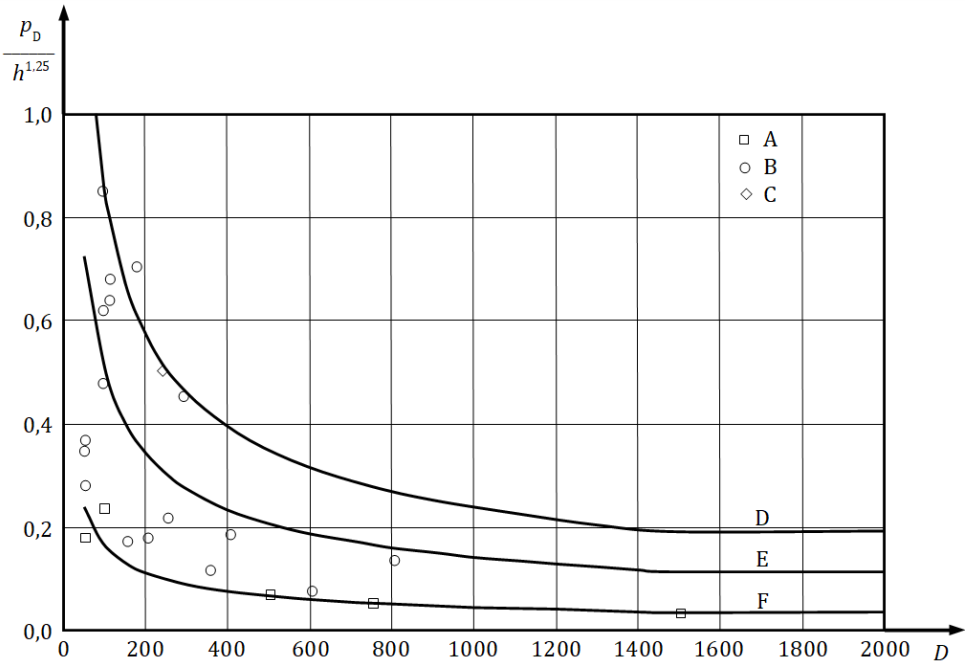

Key

A	data from Reference [163]	F	Equation 4, R = 2
B	data from Reference [164]	$p_D/h^{1.25}$	normalized ridge-building action (MN/m)
C	data from Reference [165]	D	width of thicker ice feature (m)
D	Equation 4, R = 10		
E	Equation 4, R = 6		

Figure 7. Ridge building actions versus width normalized to unit thickness of first year ice using h to the power of 1.25 (Figure A.8-21)

OVERVIEW OF LOCAL ICE ACTIONS (Clause A.8.2.5.1)

While global actions are calculated from average pressures over the nominal contact area, there can be many areas within the nominal contact area that are subjected to higher local pressures (HPZs). Consequently, global average pressures should not be used for local design and a separate consideration of local pressures is necessary. Local pressures should be used, for example, in the design of shell and stiffening elements as illustrated in Figure 9. In this revision to the standard, the illustration of local pressure in Figure 9 and consideration for design has been clarified with additional detail concerning structure grillage. It is noted however that this is for illustration, and that the designer should consider the range of possibilities for local pressure application, for plating, main frames (or stiffeners), stringers, and web frames.

Key

A global interaction area (grows with increase crushing)
B frames
C stringers
D local area for plate design
E local area for frame design
F local area for stringer design
a loaded height
w_L loaded width

Figure 9. Definition of loaded areas for local actions, example for a transversely-framed structure (Figure A.8-24)

PROBABILISTIC MODELING OF LOCAL ICE PRESSURES

Short-duration interactions with fixed and floating (Clause A.8.2.5.3.1)

A probabilistic local pressure model Jordaan et al. (1993) developed from ship impact data with MY ice floes can be applied for relatively short duration interaction events (i.e. on the order of seconds) with icebergs, bergy bits or MY fragments or any other ice impacts with fixed structures and floating systems. The model gives a probability distribution for the maximum annual pressure corresponding to an annual equivalent exposure as

$$F_p(\mathrm{p}) = \exp[\mu \exp(-p/\alpha)] \quad (5)$$

$\alpha = B_P A^{-0.7}$ modeling decreasing pressure with increasing local area

$\mu = {}^{v\,r\,t}/_{0.7}$

which for annual maximum local design pressure (mega pascals) can be written as :

$$p = x_0 + \alpha\{-\ln[F_P(p)] + \ln\mu\}$$

where

B_P is an empirical coefficient representing ice strength (MPa);
μ is the annual exposure factor (annual number of equivalent impact events);
v is the number of MY ice floe interaction events;
r represents the probability of hitting a panel given an event (0.5 in Kigoriak analysis, a value of 1 can be used to provide some measure of conservatism such as for the use of these relationships for iceberg impact, unless an alternative value can be justified);
t is the mean interaction time, expressed in seconds;
x_0 is a constant, typically zero;
0.7 represents the average duration in seconds for the Kigoriak rams.

In the earlier standard, the empirical coefficient B_P was fixed as unity (1), whereas in the current edition, variability in B_P from different ship ramming trials is given (see Figure 10). B_P = 1.25 represents aggressive Kigoriak ramming trials with MY ice (Jordaan et al.1993). This variability in ice strength demonstrates the benefit in collecting region specific data.

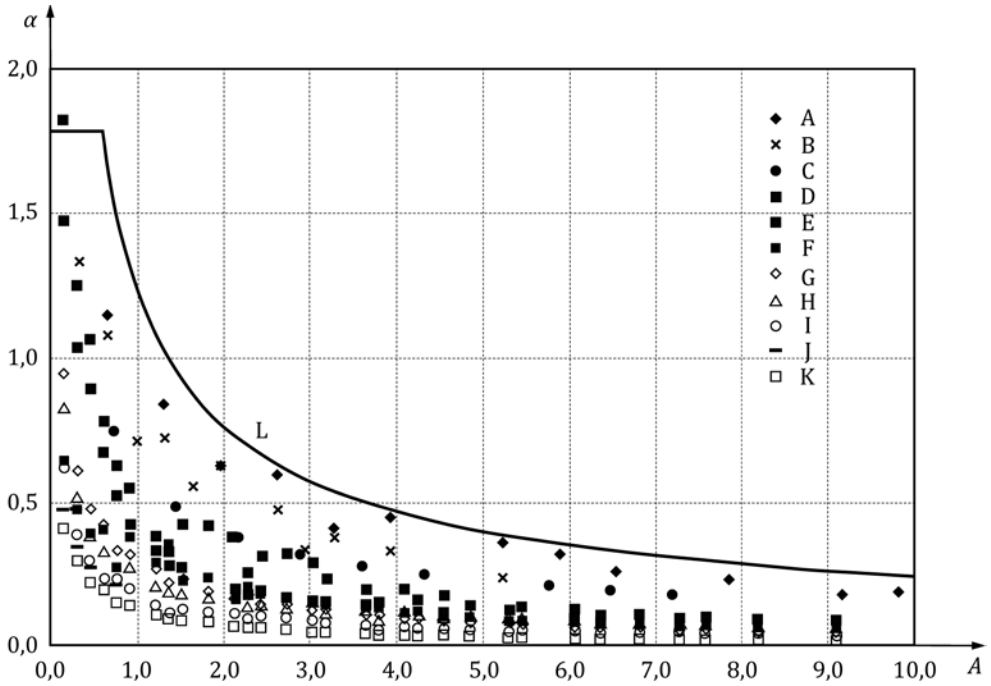

Key

A Oden
B Terry Fox
C Louis St. Laurent
D Polar Sea, Beaufort Sea 1982
E Polar Sea, N. Chukchi Sea 1983
F Polar Sea, N. Bering Sea 1983
G Polar Sea, Beaufort Sea 1984
H Polar Sea, S. Chukchi Sea 1983
I Polar Sea, Antarctica 1984
J Polar Sea, S. Bering Sea 1983
K Polar Sea, Bering Sea 1986
L original design curve based on Kigoriak, $\alpha = 1.25\ A^{-0.7}$
A local contact area, expressed in square metres
α is the local pressure parameter

Figure 10. Local pressure parameter α vs local contact area A for Oden, Terry Fox and Polar Sea ship ram trials (Taylor et al. 2009) (Figure A.8-26)

Long-duration interactions with wide structures (Clause A.8.2.5.3.2)

A new clause has been added to model long duration interactions from continuous MY interaction with fixed wide structures (e.g. platform Molikpaq). For these longer duration continuous interaction events, Jordaan et al. (2010) found that 10 min (i.e. 600 s) of continuous MY ice exposure with a wide structure was equivalent to one ram of the kind in the Kigoriak trials. Recognizing that ice crushing occurs in localized regions for only a small proportion of the total duration, Equation 5 (A.8-77) applies with the following parameters

$$\alpha = B_P A^{-0.7} \qquad (6)$$

$$\mu = {}^{vt}/_{600}$$

where

B_P is an empirical coefficient, equal to 1.25;
v is the number of MY ice floe interaction events;
t is the mean duration of each event, expressed in seconds.

It is noted that the model and specifically estimation of v reflects speeds observed during measurements of ice interaction with the Molikpaq platform.

LOCAL PRESSURES FOR THICK MASSIVE ICE FEATURES (Clause A.8.2.5.4)

In the earlier standard, the deterministic expression for local pressures on thick massive ice features having a thickness in excess of 1.5 m was given by Equation 7 (A.8-82) and illustrated in Figure 11 (see Masterson et al. 2007).

$$p_L = 7.4A^{-0.7} \quad \text{For } A \leq 10\text{m}^2 \qquad (7)$$
$$= 1.54 \quad \text{For } A > 10\text{m}^2$$

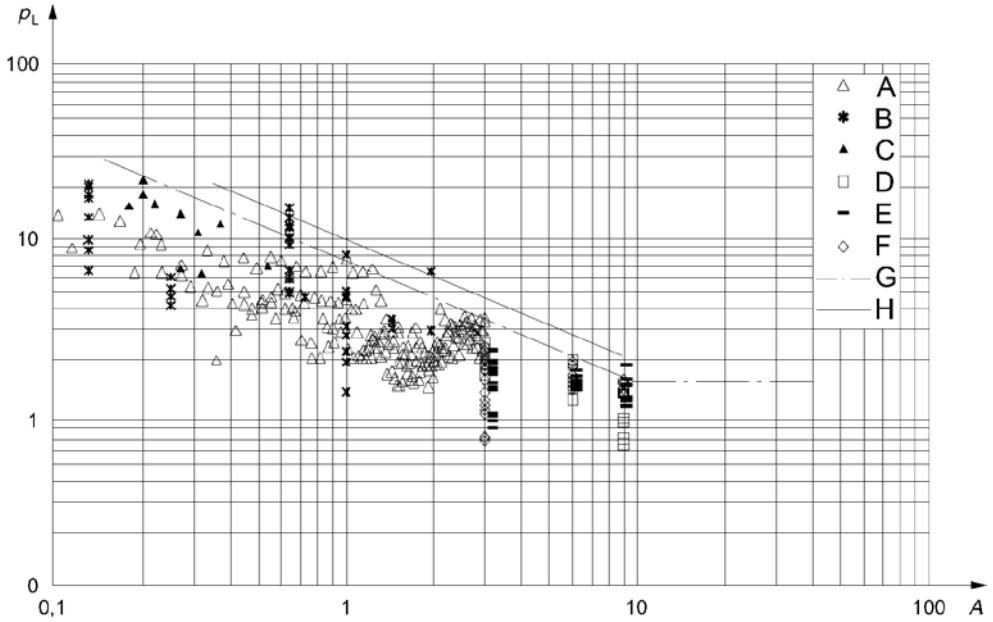

Key

A 3m^2 Pond Inlet test data
B flat jack test data
C 1989 Hobsen's Choice test data
D Molikpaq BW data
E Molikpaq N face data
F Molikpaq E face data
G $p_L = 7.4A^{-0.7}$; A ≤ 10m^2; mean plus three standard deviation; **4 equivalent rams per year**
H $p_L = 9.6A^{-0.7}$; A ≤ 10m^2; **22 equivalent rams per year**
p_L local ice pressure (MPa)
A local contact area, expressed in square metres

Figure 11. Compilation of data for ice pressures as a function of the loaded area (Masterson et al. 2007) (Figure A.8-28)

In the latest edition of the standard, basis for Equation 7 is documented (i.e. the mean plus three times the standard deviation of the data binned according to contact area). It is too noted that the probability of exceedance for three times the standard deviation, assuming the data are normally distributed, is 0.13 %. If a 1 % exceedance is applied to the data in Figure 10, a quantile regression analysis (Spencer and Morrison, 2014) yielded the corresponding Equation for local pressure as

$$p_L = 9.6A^{-0.74} \quad \text{For } A \leq 10\text{m}^2. \qquad (8)$$

It is further noted that these data are a mixture of different tests with different exposures. Since standard aims to satisfy EL and AL ice actions at annual exceedance probabilities of 10^{-2} and 10^{-4}, it should be understood that Equation 7 (A.8-82) and 8 (A.8-83) only represent exceedance probabilities ***on the pressure data*** and not values for EL actions. EL and AL values

should consider time and the maximum number of interactions in a year as illustrated with lines G and H in Figure 11.

Local Ice Pressure Combinations (Clause A.8.2.5.5)

This clause addresses the simultaneous application of background ice pressures outside of the areas where local ice pressures are applied for local design of the structure as illustrated earlier in Figure 9. In application of this clause, the relationship between local HPZ pressures (which vary in magnitude, space and time) and global forces (and pressures) is defined. The global force at any instant in time through an interaction event is the sum of the local HPZ forces averaged over the nominal contact area. Ideally, a designer would model the distribution of HPZs over some nominal contact area directly (Ralph, 2016 and Ralph and Jordaan, 2017), but in the absence of such a model, we apply the approach in Figure 12 and Equation 9 (A.8-84) given as

$$p_0^P = \frac{p_0 A_0 - p_L A_L}{A_0 - A_L}. \quad (9)$$

Using this equation, a local ice pressure, p_L, is applied over a local area, A, while there can be a lower ice pressure, p_0, over a much larger portion of the structure with an area, A_0. Note that the ice pressure, p_L, the total pressure over the local area, is not added to p_0.

It is clarified in this clause that in practice, peak global actions and peak local pressures are unlikely to occur at the same instant in time, and the use of an EL value for the local ice pressure, p_L, with an EL value for the surrounding (or global) ice pressure, p_0, will lead to an overly-conservative design. The designer is encouraged to use available and relevant data to justify more realistic background ice pressures such as HPZ modeling noted above.

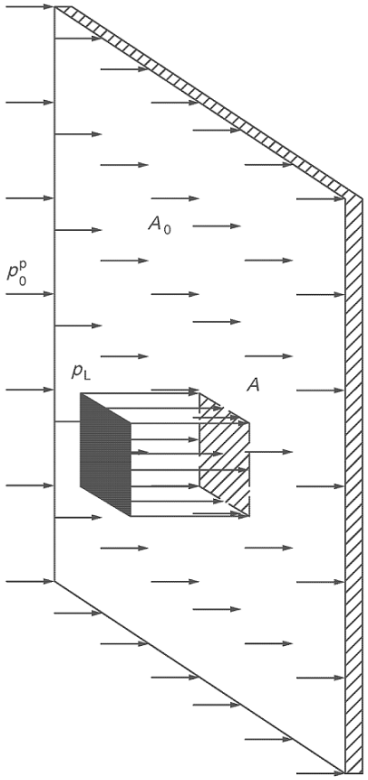

Key

p_L pressure patch
A local contact area, expressed in square metres
p_0^P background ice pressure
A_0 background area

Figure 12. Method of combining the local ice pressure with a pressure acting on a larger area (Figure A.8-29)

CONCLUSIONS

Significant changes are made to the global and local ice actions clauses of the ISO19906 standard to include greater clarity and transparency in guiding the designer to appropriate EL and AL design actions; whether the designer chooses deterministic or probabilistic approaches. Exposure is specifically addressed recognizing that designs can vary depending on the region, the time of year, and how system is operated. With an understanding of the corresponding environmental conditions, design ice actions can be estimated. While expert judgement is extremely valuable, the designer can have greater confidence in his design decisions having comprehensively modeled variability in environmental conditions (i.e. particularly when design life exceeds the extent of measurements and extrapolation is necessary). Besides exposure, many design formulations including level ice and multi-year ridge loads on sloping and conical structures, as well as limit forces from ridge building actions have been updated based on recent experiments, analysis and verification exercises.

ACKNOWLEDGEMENTS

A sincere thanks to my committee members who ultimately made this initiative possible: Tom Brown (University of Calgary), Jim Bruce (Chevron), Dan Fenz (ExxonMobil), Fengwei Guo (DNV-GL), Ivan Metrikin (Equinor), Naoki Nakazawa (Systems Engineering Associates), Paul Spencer (Ausenco), Dev Sodhi (CREEL), and KimThow Yap (KOMTech). A special thanks also to Bob Frederking and Richard McKenna.

REFERENCES

Bjerkas, M. & Nord, T., 2016. Ice action on Swedish lighthouses revisited. *Proceeding of the 23nd IAHR International Symposium on Ice*.

Croasdale, K, Frederking, R., Wright, B. & Comfort, G., 1992. Size effect on pack ice driving forces, *Proceeding of the 11th IAHR International Symposium on Ice*. pp.1481-1496.

Croasdale, K., Brown, T.G., LI, G., Spring, W., Fuglem, M. & Thijjsen, J., 2018. The Action of Long Multiyear Ridges on Upward Sloping Conical Structures, *Cold Regions Science and Technology*, Vol. 154, pp. 166-180.

Croasdale, K., Brown, T.G., LI, G., Spring, W., Fuglem, M. & Thijjsen, J., 2018. The Action of Short Multiyear Ridges on Upward Sloping Conical Structures, *Cold Regions Science and Technology*, Vol. 154, pp.142-154.

Croasdale, K.R., 2009. Limit force ice loads: an update, *Proceeding of the 20th International Conference on Port and Ocean Engineering under Arctic Conditions*, pp 230-239.

Croasdale, K.R., Brown, T.G., LI, G., Spring, W., Fuglem, M. & Thijjsen, J., 2016. The interaction of multi-year ridges with upward sloping structures, *Arctic Technology Conference*, paper OTC 27426.

Jefferies, M., Kärnä, T. & Løset S., 2008. Field data on the magnification of ice loads on vertical structures, *Proceeding of the 1st IAHR International Symposium on Ice*, pp.1115–1133.

Jordaan, I. J., Bruce, J., Masterson, D., & Frederking, R., 2010. Local ice pressures for multiyear ice accounting for exposure, *Cold Regions Science & Technol.*, Vol.61, pp. 97–106.

Jordaan, I.J., Maes, M.A., Brown, P. & Hermans, I., 1993. Probabilistic Analysis of Local Ice Pressures, *Journal of Offshore Mechanics and Arctic Engineering*, Vol. 115, pp.83–89.

Kärnä,, T. & Qu, Y., 2006. *Analysis of the size effect in ice crushing*, Edition 2. VTT Technical Research Centre of Finland, Internal Report RTE-IR-6/2005.

Kärnä,, T., Qu, Y. & Yue, Q.J., 2006. Extended Baltic model of global ice forces, *Proceeding of the 18th IAHR International Symposium on Ice*, pp.261-268.

Määttänen, M. & Kärnä, T. 2011. ISO 19906 ice crushing load design extension for narrow structures, *Proceeding of the 21th International Conference on Port and Ocean Engineering under Arctic Conditions*. pp. 47 – 51

Masterson, D., Frederking, B., Wright, B., Karna, T. & Maddock, W. A., 2007. Revised pressure area curve, *Proceeding of the 19th International Conference on Port and Ocean Engineering under Arctic Conditions*, pp. 305–314.

Masterson, D.M., 2011. *Nevel method for multi-year ice ridge load calculation*, Chevron Canada report.

Nevel, D., 1992. *Unpublished, Ice forces on cones from multiyear ridges,* 1992.

Palmer, A. & Croasdale, K., 2013. *Arctic Offshore Engineering*. World Scientific Publishing, Singapore.

Paquette, E. & Brown, T.G., 2017. Ice crushing forces on offshore structures: Global effective pressures and the ISO 19906 design equation, *Cold Regions Science and Technology,* 142, p. 55–69.

Ralph, F., 2016. *Design of Ships and Offshore Structures: A Probabilistic Approach for Multi-Year Ice and Iceberg Impact Loads for Decision-making with Uncertainty*. A Thesis submitted to the School of Graduate Studies for the degree of Doctor of Philosophy. Faculty of Engineering and Applied Science, Memorial University.

Ralph, F. & Jordaan, I., 2017. Local Design Pressures During Ship Ram Events Modeling the Occurrence and Intensity of High Pressure Zones. *Proceeding of the ASME 37th International Conference on Ocean, Offshore Mechanics and Arctic Engineering*, OMAE2017-62545..

Sandwell, 1994. *Processing of pack ice stress data,* Sandwell Report 113027 submitted to National Research Council, Ottawa.

Spencer, P. & Morrison, T., 2014. Quantile regression as a tool for investigating local and global ice pressures, *Arctic Technology Conference*, OTC paper 24550.

Taylor, R., Jordaan, I., LI, C. & SUDOM, D., 2009. Local Design Pressures for Structures in Ice: Analysis of Full-Scale Data, *Journal of Offshore Mechanics and Arctic Engineering* 132, no. 3, Paper 031502, 2010, doi:10.1115/1.4000504.

Thijjsen, J. & Fuglem, M., 2015. Methodology to evaluate sea ice loads for seasonal operations, *Proceeding of the ASME 34th International Conference on Ocean Offshore Mechanics and Arctic Engineering*.

Thijjsen, J., Fuglem, M., & Croasdale, K.R., 2016. Probabilistic assessment of multi-year sea ice loads on upward sloping arctic structures, *Proceedings of Arctic Technology Conference*, OTC paper 27364.

Wang, Z., Muggeridge, D.B., & Croasdale, K.R., 1997. Ridge ice loads on proposed faceted conical structures, *Proceeding of the 7th International Offshore and Polar Engineering Conference*.

Wright, B.D., Frederking, R. & Croasdale, K.R., 1992. Pack ice driving forces inferred from the Molikpaq ice loads. *Proceeding of the IAHR International Symposium on Ice*, pp.1468-1480